IOP Publishing Classical and Quantum Gravity

Class. Quantum Grav. **37** (2020) 035002 (30pp) https://doi.org/10.1088/1361-6382/ab5c94

Asymptotic states of black holes in KMY model

Pei-Ming Ho[1], **Yoshinori Matsuo**[1,2] **and Shu-Jung Yang**[1]

[1] Department of Physics and Center for Theoretical Physics, National Taiwan University, Taipei 106, Taiwan, Republic of China
[2] Department of Physics, Osaka University, Toyonaka, Osaka 560-0043, Japan

E-mail: pmho@phys.ntu.edu.tw, matsuo@het.phys.sci.osaka-u.ac.jp and r05222083@ntu.edu.tw

Received 15 June 2019, revised 22 November 2019
Accepted for publication 28 November 2019
Published 13 January 2020

Abstract

Following the work of Kawai, Matsuo and Yokokura, we study the dynamical collapsing process with spherical symmetry in the time-dependent space-time background including the back-reaction of Hawking radiation. We show that in this model there are two classes of asymptotic solutions. One of the two classes is known previously. These states have the slope $\partial a/\partial r$ approximately equal to 1. The other class of asymptotic solutions is that of shells with a small thickness. We emphasize that these thin shells should be properly understood as configurations in the low-energy effective theory. They behave characteristically differently from the singular states of ideal thin shells of zero thickness.

Keywords: black hole, gravitational collapse, Hawking radiation

(Some figures may appear in colour only in the online journal)

1. Introduction

In the study of the black holes, it is common practice to study the formation and evaporation of a black hole separately as independent processes for the simplicity of calculation. During the formation process, which is typically treated as a purely classical process, classical matter collapses and an event horizon appears. After that, the evaporation process due to the quantum effect is considered as an independent process. In this approximation scheme, the evaporation is computed in the presence of the event horizon of a classical black hole with a constant Schwarzschild radius.

Of course, in reality, the Schwarzschild radius must decrease over time if the black hole completely evaporates in the end. But some people argued that the extremely slow change in

the Schwarzschild radius can be ignored for the study of the black-hole evaporation. As a test of the robustness of these arguments, one should check whether the evaporation is significantly modified if the time-dependence of the Schwarzschild radius is turned on.

This was done in the paper of Kawai *et al* [1]. (See also [2–8].) The formation and evaporation of a black hole is viewed as a single process, and the back-reaction of Hawking radiation on the geometry is included from the very beginning of the black-hole formation. The Schwarzschild radius is time-dependent due to Hawking radiation.

It turns out that, as the vacuum energy-momentum tensor is assumed to be dominated by the Hawking radiation outside the collapsing matter in this model, when the collapsing matter has a smooth density distribution, it completely evaporates without apparent horizon [1]. In contrast, an ideal thin shell with a delta-function energy density does not evaporate completely. Instead, it approaches a classical black hole in the infinite future with an event horizon [1].

There are a few obvious questions. For example, is the ideal thin shell of delta-function energy distribution physical? Are there other classes of behaviors characteristically different from the two classes of solutions already found in [1]? These are the questions that motivated this research project.

In this paper, we first discuss the difference between the thin shell with delta function energy distribution and that with a finite but very small thickness. These two shells are expected to be almost indistinguishable. However, they have characteristically different behaviors in calculations of the Hawking radiation. We shall demonstrate the difference by comparing a thin shell with a thickness of the Planck scale and a shell with a delta function energy distribution. While the latter survives in the end as a classical black hole, the former evaporates completely within finite time. Thus, the thin shell with delta function density distribution is unphysical, and hence we will focus on the configurations with a finite thickness no less than the Planck scale.

Then, we will show that there are at least two classes of asymptotic behaviors of the collapsing matter as a result of the back-reaction of Hawking radiation[3]. One of the two classes has already been proposed and studied in [1] and [2–8]. The other class is described as a thin shell in the low-energy theory, and it should be distinguished from the ideal thin shell of zero thickness. We will examine the details of both classes of collapsing processes in this paper through both analytical study and numerical simulation.

The plan of this paper is as follows. In section 2, we briefly review the KMY model. In section 3, we examine the notion of thin shells in the context of low-energy effective theories. We argue that it is inappropriate to apply the low-energy theory to ideal thin shells of zero thickness, as their behavior is characteristically different from thin shells of a small but finite thickness. In section 4, we consider shells with an energy distribution for which the slope $\partial a/\partial r \simeq 1$. These configurations are particularly interesting as asymptotic states [1]. Excluding the unphysical ideal thin shells, in section 5, we argue that there are two types of asymptotic states, the slope-1 states and the thin shell states. This claim is backed up by numerical simulation presented in section 6. Finally, we conclude in section 7.

2. Review of KMY model

We will refer to the approach of [1], which is followed by [2–8], as the KMY model. One of the crucial points of this approach is that the back-reaction of Hawking radiation to the

[3] Recall that 2D black holes are also categorized as two classes. It was shown in [9] that an apparent horizon will either appear or be absent depending on the magnitude of the ingoing energy flux.

geometry is taken into account. But the importance of the back-reaction of Hawking radiation, or that of the vacuum energy-momentum tensor, has been considered before the KMY model [10–14] in the literature. (See also [15–20] for later proposals.) Another crucial feature of the KMY model is that it further assumes that the vacuum energy-momentum tensor is dominated by Hawking radiation.

Unlike most of the models of black holes, the null energy condition is not violated in the KMY model, and this is directly related to the absence of the apparent horizon. (See e.g. [21].) Strictly speaking, the violation of the null energy condition in conventional models of black holes is based on a few assumptions. For instance, it is often considered as a consequence of the equivalence principle. However, in general, the quantum states cannot be defined locally. Instead, they depend on the boundary conditions. The quantum state of the black hole can break the local equivalence principle, and the vacuum energy-momentum tensor should be determined by a specific quantum field theory which has a consistent UV limit including quantum gravity. It is not clear whether certain important quantum gravity effects are missing from the quantum field theories people usually consider in their models. Furthermore, as it was pointed out in [22], there must be 'drama' at the horizon for the information to be preserved, as it was also argued in [23].

Our viewpoint is that the quantum state breaks the equivalence principle to admit unitarity for a UV-complete theory. The vacuum energy-momentum tensor obviously depends on the matter content of the model. While the vacuum energy-momentum tensor is typically calculated in some simplified models of matter fields (e.g. two dimensional massless scalar fields of s-wave approximation in [24]) in the conventional model, the KMY model simply assumes the vacuum energy-momentum tensor to be dominated by the outgoing positive energy flux (i.e. the Hawking radiation) as an alternative. It turns out that, as a consequence of the semi-classical Einstein equation, a pressure at the Planck scale [2] appears on the collapsing shell as an effective 'firewall'. This is consistent with the analysis of [25], which shows that a pressure-less thin shell is inconsistent with the absence of horizon, and in agreement with [26], which says that either pressure or charges are necessary to keep the shell null.

While there is no good reason to strictly preserve the null energy condition in a quantum field theory for all quantum states, it may be only weakly violated to the extent that the KMY model is still a good approximation. (See [8] for a generalization of the KMY model with a more general vacuum energy-momentum tensor.) To say the least, the KMY model is an interesting alternative to conventional models of black holes that may provide a self-consistent story including quantum effects.

In this paper, we are interested in the asymptotic configurations in the KMY model. It was shown in [1] that there would be no event or apparent horizon[4] for a certain smooth configuration, which will be referred to as the 'slope-1' configuration in this paper[5]. In fact, it can be proven [3, 5] that there is no apparent horizon as long as the collapsing matter completely evaporates within a finite time. According to the semiclassical Einstein equation, the Schwarzschild radius shrinks with time in a superluminal fashion due to the loss of energy into Hawking radiation. As a result, the collapsing matter can never fall through the Schwarzschild radius, as long as the (incipient) black hole evaporates completely within finite time [1, 3].

An exceptional configuration for the collapsing matter that does not evaporate within a finite time is the case of the thin shell with an energy density given by the Dirac delta function.

[4] The possibility that black holes have no horizon has also been proposed by many others. For an incomplete list, see [12, 13, 15, 16, 27–36].

[5] It was called an 'asymptotic black hole' in [7].

Its Hawking radiation decreases with time so that the black hole survives in the infinite future, and an event horizon arises like a classical black hole [1].

Notice that the time evolution of a thin shell of absolutely zero thickness may or may not be obtained by the zero thickness limit from a thin shell of finite thickness, as the equation determining Hawking radiation involves higher derivatives. We investigate in this paper whether small (Planck-scale) deviations from the mathematical notion of a perfect zero-thickness thin shell would lead to characteristically different space-time structures at large scales.

Another specific question we would like to answer is whether the smooth configuration studied in [1] (called the 'slope-1' configuration) is the only asymptotic limit for generic initial states. We shall find that there is another class of asymptotic configurations.

2.1. Metric

A generic, spherically symmetric 4D metric can be put in the following form in the outgoing Eddington–Finckelstein coordinate

$$\mathrm{d}s^2 = -\mathrm{e}^{2\psi(u,r)}\left(1-\frac{a(u,r)}{r}\right)\mathrm{d}u^2 - 2\mathrm{e}^{\psi(u,r)}\mathrm{d}u\mathrm{d}r + r^2\mathrm{d}\Omega^2, \tag{1}$$

which involves two parametric functions $\psi(u,r)$ and $a(u,r)$. The time evolution of this metric will be studied in terms of the Eddington retarded time u. Due to spherical symmetry, the functions $\psi(u,r)$ and $a(u,r)$ only depend on u and the areal radius r.

At any given instant of time u, the function $a(u,r)$ in the metric (1) gives twice the Bondi mass inside the ball of the radius r centered at the origin. The other function $\psi(u,r)$ in the metric (1) is the exponent of the redshift factor $\mathrm{e}^{\psi(u,r)}$ between the retarded time coordinate u at spatial infinity and the retarded time coordinate $\hat{u}(u,r)$ at r [7].

The metric (1) is only suitable for the region $r > r^*(u)$, where $r^*(u)$ is the (largest) solution to the equation $r^*(u) = a(u, r^*(u))$. It is also only valid outside the apparent horizon. As the apparent horizon appears in most models of black holes, the metric (1) is often considered inappropriate, and so the coordinate system using the (v,r) coordinates (with the ingoing Eddington–Finckelstein coordinate) is more commonly used in the literature. However, as we mentioned in the introduction, there is no apparent horizon in the KMY model, as a consequence of the non-violation of the null energy condition, as opposed to the conventional model. (It has been shown in [6, 21] that the null energy condition has to be violated for the existence of the apparent horizon.) In any case, one can use any metric until a (coordinate) singularity appears. The metric (1) will turn out to be convenient in the discussion below for the KMY model.

We assume that the collapsing matter has an outer radius $R_0(u)$ beyond which there is no ingoing energy flux (but there can be outgoing energy flux as Hawking radiation), so that $a(u,r)$ is r-independent outside the outer radius $R_0(u)$:

$$a(u,r) = a_0(u) \quad \text{for} \quad r \geqslant R_0(u) \tag{2}$$

for some function $a_0(u)$ which is twice the total Bondi mass of the collapsing matter.

When $a_0(u)$ is time-independent, as in the classical case without Hawking radiation, the metric (1) is equivalent to the Schwarzschild metric with Schwarzschild radius a_0 for $r > R_0(u)$. When $a_0(u)$ is not time-independent, there is outgoing energy flux for $r > R_0(u)$ given by

$$T_{uu} = -\frac{1}{\kappa r^2}\frac{\mathrm{d}a_0(u)}{\mathrm{d}u}, \tag{3}$$

where $\kappa = 8\pi G_N$ and G_N is the Newton constant. This outgoing energy flux is used to represent Hawking radiation and is assumed to be positive, so that the Schwarzschild radius $a_0(u)$ decreases over time and $\mathrm{d}a_0/\mathrm{d}u < 0$.

For simplicity, in this paper, we shall assume that the collapsing matter is falling at the speed of light. Applying the general results of [7] to this special case, the redshift factor $\mathrm{e}^{\psi(u,r)}$ is given by

$$\psi(u,r) = -\int_r^\infty \mathrm{d}\bar{r}\, \frac{\frac{\partial a(u,\bar{r})}{\partial \bar{r}}}{\bar{r} - a(u,\bar{r})}. \tag{4}$$

Because of equation (2), $\psi(u,r) = 0$ for $r > R_0(u)$.

According to equation (4), the redshift factor for the retarded time U of the Minkowski space inside the collapsing matter is

$$\log\left(\frac{\mathrm{d}U(u)}{\mathrm{d}u}\right) = \psi_0(u) = -\int_0^{R_0(u)} \mathrm{d}r\, \frac{\frac{\partial a(u,r)}{\partial r}}{r - a(u,r)}. \tag{5}$$

Since $a(u,r)$ is always a monotonic function of r in the range of integration in equation (5), a can be used as a coordinate in place of r to parametrize the integral, hence the integral (5) can also be expressed as

$$\psi_0(u) = -\int_0^{a_0(u)} \frac{\mathrm{d}a}{r(u,a) - a}. \tag{6}$$

One may wonder if $\psi_0(u)$ diverges in the limit $r \to a$. It is impossible as long as there is no divergence in the Hawking radiation, as we will discuss later in the paragraph below equation (19). This also means that r can never coincide with a, and thus there would be no apparent horizon.

2.2. Hawking radiation

The Hawking radiation is created during the gravitational collapse because the quantum vacuum state of incoming matter in the infinite past evolves to a state that is no longer the vacuum state at large r after the gravitational collapse. We shall adopt the formula for Hawking radiation of [1], which is in agreement with that of [24, 37], although the rest of the vacuum energy-momentum tensor is omitted.

Following these works, approximating the vacuum energy-momentum tensor by that of s-wave modes of massless scalar fields, and assuming that the initial state in the infinite past is the Minkowskian vacuum state, the Hawking radiation is given by the energy flux

$$T_{uu} = \frac{\mathcal{N}}{4\pi r^2}\{u, U(u)\}, \tag{7}$$

where $\kappa = 8\pi G$, $\mathcal{N}$ is a numerical constant proportional to the number of massless fields in Hawking radiation and $\{u, U(u)\}$ is the Schwarzian derivative defined by

$$\{u, U(u)\} \equiv \left[\frac{\frac{\mathrm{d}^2U(u)}{\mathrm{d}u^2}}{\frac{\mathrm{d}U(u)}{\mathrm{d}u}}\right]^2 - \frac{2}{3}\frac{\frac{\mathrm{d}^3U(u)}{\mathrm{d}u^3}}{\frac{\mathrm{d}U(u)}{\mathrm{d}u}}. \tag{8}$$

Using equation (5), one can rewrite the Schwarzian derivative as

$$\{u, U(u)\} \equiv \frac{1}{3}\left[\dot{\psi}_0^2(u) - 2\ddot{\psi}_0(u)\right], \tag{9}$$

where the dots denote u-derivatives.

3. Thin shells

In this section, we first review the case of an ideal thin shell, i.e. a thin shell of zero thickness. Then we compare it with the notion of a pseudo thin shell, which has a finite thickness larger than the cutoff length scale of the low-energy effective theory, but it is thin enough so that its behavior is not sensitive to the precise thickness. Their behaviors turn out to be characteristically different.

3.1. Ideal thin shell

For a thin shell of zero thickness, the function $a(u,r)$ in the metric (1) is given by

$$a(u,r) = a_0(u)\Theta(r - R_0(u)), \tag{10}$$

where $\Theta(x)$ is the step function that is 0 or 1 for $x<0$ or $x>0$. It has a diverging energy density proportional to the Dirac delta function that diverges at $r = R_0(u)$. For the low-energy effective theory to be applicable, a shell should have a finite thickness much larger than the Planck length, and an energy density much smaller than the Planck scale. However, this notion of an ideal thin shell has been widely used in the literature in the context of low-energy effective theories.

To evaluate $\psi_0(u)$, we use equation (6), with $r(u,a)$ given by inverting equation (10):

$$r(u,a) = R_0(u)\ . \tag{11}$$

Hence equation (6) can be evaluated as

$$\psi_0(u) = -\int_0^{a_0(u)} \frac{\mathrm{d}a}{R_0(u)-a} = \log\left(\frac{R_0(u)-a_0(u)}{R_0(u)}\right). \tag{12}$$

3.1.1. Background With constant Schwarzschild radius. Let us first consider the evolution of the ideal thin shell with a fixed Schwarzschild radius, ignoring the back-reaction of Hawking radiation.

The thin shell is by assumption falling at the speed of light, hence we have

$$\frac{\mathrm{d}R_0(u)}{\mathrm{d}u} = -\frac{1}{2}\frac{R_0(u)-a_0(u)}{R_0(u)} \tag{13}$$

according to the metric (1). When a_0 is assumed to be time-independent, its solution is

$$R_0(u) \simeq a_0 + C_0 \mathrm{e}^{-\frac{u}{2a_0}} \tag{14}$$

when $R_0(u) - a_0 \ll a_0$. Equation (12) then gives

$$\dot{\psi}_0(u) \simeq -\frac{1}{2a_0}, \tag{15}$$

and the Schwarzian derivative can be easily computed

$$\{u, U(u)\} = \frac{1}{3}\left(\dot{\psi}_0^2 - 2\ddot{\psi}_0\right) \simeq \frac{1}{12a_0^2}, \tag{16}$$

which gives the conventional result of Hawking radiation

$$\frac{\mathrm{d}a_0}{\mathrm{d}u} \simeq -\frac{\kappa\mathcal{N}}{48\pi a_0^2}. \tag{17}$$

As a result, the thin shell evaporates completely within a finite time of order $\mathcal{O}(a_0^3/\kappa)$.

Some people have argued that a constant background is justified as a good approximation because the time scale of the change in the Schwarzschild radius is $\mathcal{O}(a_0^3/\kappa)$, while the time-scale of the gravitational collapse is $\mathcal{O}(a_0)$; the large hierarchy in the time scales implies that the former cannot have a significant effect on the latter. This argument is not rigorous because, strictly speaking, it makes sense to compare the time scales only when both are defined with respect to the same observers. The time scale of the Schwarzschild radius is $\mathcal{O}(a_0^3/\kappa)$ for distant observers, and yet the time-scale of gravitational collapse is $\mathcal{O}(a_0)$ only for infalling observers. Classically, it takes an infinite time for distant observers to see the star falling inside the horizon, so after including the quantum effect, the time scale of gravitational collapse should also be $\mathcal{O}(a_0^3/\kappa)$ for distant observers. Indeed, we will see below that the time-dependence of the Schwarzschild radius, despite of how small it is, can have a significant effect.

3.1.2. Back-reacted background. However, as there is Hawking radiation, $a_0(u)$ must decrease over time due to the outgoing energy flux (3). Since the Hawking radiation is given by (7), the time evolution of $a_0(u)$ is given by the differential equation;

$$\frac{\mathrm{d}a_0(u)}{\mathrm{d}u} = -\frac{\kappa\mathcal{N}}{4\pi}\{u, U(u)\}. \tag{18}$$

This modification would change the evaluation of $\dot{\psi}_0(u)$ (15). Using equations (12) and (13), we find

$$\dot{\psi}_0(u) \simeq -\frac{a_0(u)}{2R_0^2(u)} - \frac{\dot{a}_0(u)}{R_0(u) - a_0(u)}. \tag{19}$$

While the first term is always finite, the 2nd term diverges at the horizon unless $\dot{a}_0(u)$ vanishes at the horizon.

As the outgoing energy flux T_{uu} of the energy-momentum tensor is identified with the Hawking radiation in the KMY model, the finiteness of T_{uu} implies, through equations (7) and (9), that $\dot{\psi}_0$ must be finite, unless its divergence cancels the divergence in the other term in equation (9). The cancellation of divergence in equation (9) demands $\dot{\psi}_0 \sim \frac{2}{c-u}$ for some constant c as $u \to c$, with the implication that $\dot{\psi}_0$ is positive when $u \to c$ (but $u < c$). However, $\dot{\psi}_0$ should be negative according to equation (5), since the factor $\mathrm{d}U/\mathrm{d}u$ should be decreasing with time. Hence it is impossible for $\dot{\psi}_0$ to blow up. Thus, it is inconsistent to have a diverging $\dot{\psi}_0$ at the horizon, hence $\dot{a}_0$ must vanish at the horizon. The conclusion is thus that once the time-dependence of the Schwarzschild radius $a(u)$ is taken into account, the ideal thin shell cannot cross the horizon without turning off Hawking radiation. Indeed, it was shown in [1] that the Hawking radiation decreases to zero and a classical black hole survives the incomplete evaporation for a collapsing ideal thin shell.

More explicitly, assuming that $a_0(u)$ changes very slowly, equation (13) implies that the shell asymptotes to the Schwarzschild radius $r = a_0(u)$. When the shell is sufficiently close to the Schwarzschild radius $R_0(u) \simeq a_0(u)$, equation (18) is solved with [1]

$$u \simeq \frac{\mathrm{e}^{-\frac{D^2}{2}}}{6\pi B}\int_D^\xi \mathrm{d}\xi'\, \mathrm{e}^{\frac{\xi'^2}{4}}, \tag{20}$$

$$a(u) \simeq a(0) - B \int_D^{\xi} \mathrm{d}\xi' \, \mathrm{e}^{-\frac{\xi'^2}{4}}, \tag{21}$$

for constant parameters B and D. This solution describes a decaying Hawking radiation that vanishes at the event horizon, and the ideal thin shell is only partially evaporated. See [1] also for numerical simulation.

To be more precise, the collapsing shell exponentially approaches the shell as described by equation (14) for constant Schwarzschild radius when the back-reaction from Hawking radiation is ignored. In the back-reacted geometry, equation (14) is modified as

$$R_0(u) \simeq a_0(u) + C_0 \mathrm{e}^{-\frac{u}{2a_0(u)}} - 2a_0(u)\dot{a}_0(u) \, . \tag{22}$$

As $\dot{a}_0(u) \leqslant 0$, the shell cannot reach the Schwarzschild radius unless $\dot{a}_0(u) \to 0$ [1]. By using the conventional formula of the Hawking radiation, $\dot{a}_0 = -\sigma/a_0^2$, the minimum distance after a long time would be

$$R_0(u) \simeq a_0(u) + \frac{2\sigma}{a_0(u)} \, . \tag{23}$$

This argument is generalized in [36] to the general metric (1) with finite and continuous $\psi(u, r)$ and with positive definite $a(u, r)$ before the complete evaporation. (See the reference for more detailed conditions on the geometry.)

To summarize, for the ideal thin shell, if we ignore the time-dependence of the Schwarzschild radius, the black hole would completely evaporate as in the conventional model, but if we account for the time dependence of the Schwarzschild radius, the black hole would not evaporate completely. While one may suspect that certain omitted details of the quantum effect involved in this process could further change the conclusion, it is, to say the least, an example showing that the back-reaction of Hawking radiation has the potential to play a crucial role. Calculations without back-reaction need to be further justified.

3.2. Pseudo thin shell

Here we discuss the notion of a 'pseudo thin shell' in the context of the low-energy effective theory with a cutoff length scale ℓ larger than the Planck length ℓ_p. It turns out that the behavior of the pseudo thin shell is characteristically different from the ideal thin shell (when the time-dependence of the background is turned on). This means that we cannot trust the low-energy effective theory on its description of the ideal thin shell. In the context of low-energy effective theories, the notion of the ideal thin shell should be viewed as invalid.

The purpose of this subsection is to point out the fact that the ideal thin shell is over-sensitive to details at the Planck scale. For this purpose, we do not have to justify our choice of the profile for the pseudo thin shell. Nevertheless, the pseudo thin shell is a natural consideration as an interpolation between the ideal thin shell and the slope-1 configuration described in the next section.

It was pointed out in [1] that the Hawking radiation from a single ideal thin shell and that from the continuum limit of infinitely many shells (the slope-1 configuration) are very different. This may seem weird at first sight since the slope-1 configuration was constructed as a collection of many thin shells. The reason behind is that the ideal thin shell has pathological behavior due to higher-derivative terms in its evolution equation, which can be removed in a suitable continuum limit.

When we model a smooth configuration as a large (but finite) number of thin shells in numerical simulation, it is better to consider a collection of pseudo thin shells (instead of ideal thin shells) to avoid the pathological behaviors of ideal thin shells. In terms of pseudo thin shells, that there is no drastic difference between the Hawking radiation for a single (pseudo thin) shell and that for a configuration of many thin shells (e.g. the slope-1 configuration). We will have more discussions on the pseudo thin shell in the next subsection.

Here, we consider the pseudo thin shell with the following profile;

$$a(u,r) \simeq \left(r - \frac{2\sigma}{r}\right)\left[\Theta(r - R_i(u)) - \Theta(r - R_0(u))\right] + a_0(u)\Theta(r - R_0(u)), \tag{24}$$

where R_0 and R_i are the outer and inner radii, and $R_0(u) - R_i(u)$ is assumed to be much smaller than $R_0(u)$. This pseudo thin shell still contains an ideal thin shell at the innermost surface. While this does not interfere with our purpose to show that a small deviation from an ideal thin shell makes a large difference, the difference between an ideal thin shell only at the innermost surface and a finite-density distribution everywhere is negligible since physics at the innermost part is almost irrelevant due to the large redshift factor as we will see soon.

The Schwarzschild radii at the outer and inner surfaces of the shell are thus

$$a_0(u) \equiv R_0(u) - \frac{2\sigma}{R_0(u)}, \tag{25}$$

$$a_i(u) \equiv R_i(u) - \frac{2\sigma}{R_i(u)}. \tag{26}$$

These formulas, together with the assumption that the shells are collapsing at the speed of light, imply that the Schwarzschild radii $a(u)$ change with time according to the conventional formula of Hawking radiation $\dot{a} \simeq -\sigma/a^2$ for some constant σ. In comparison with equation (17), σ is a constant parameter of the Planck scale

$$\sigma \simeq \frac{\kappa\mathcal{N}}{48\pi} \sim \mathcal{O}(\ell_{\rm P}^2), \tag{27}$$

where $\mathcal{N}$ was defined in equation (7). We shall compare the rates of evaporation for a pseudo thin shell and an ideal thin shell, taking into consideration the time-dependence of the Schwarzschild radius.

Within the shell ($r \in (R_i(u), R_0(u)]$), except for the innermost surface of the shell, this is the same profile as the smooth configuration proposed in [1], which will be discussed below in section 4. But at the same time, at a length scale much larger than the thickness $\Delta R \equiv R_0(u) - R_i(u)$, its profile is essentially the same as that of the ideal thin shell.

For this configuration (24), we have

$$\begin{aligned}\psi_0(u) &\simeq \log\left(\frac{R_i(u) - a_i(u)}{R_i(u)}\right) - \frac{R_0^2(u) - R_i^2(u)}{4\sigma} \\ &\simeq \log\left(\frac{\sigma}{R_i^2(u)}\right) - \frac{R_0^2(u) - R_i^2(u)}{4\sigma} \simeq -\frac{R_0^2(u) - R_i^2(u)}{4\sigma},\end{aligned} \tag{28}$$

where in the last line we have assumed that

$$\Delta R(u) \equiv R_0(u) - R_i(u) \gg \frac{2\sigma}{R_i(u)} \log\left(\frac{R_i^2(u)}{\sigma}\right). \tag{29}$$

Notice that, since σ is of the order of the Planck length squared, the inequality above is satisfied even when $\Delta R \equiv R_0(u) - R_i(u)$ is as short as a Planck length if $R_i^2(u) \gg \sigma$. This difference $\Delta R(u)$ in the areal radius corresponds to a thickness of the shell

$$\Delta L \simeq \sqrt{g_{rr}(R_0(u))}\Delta R(u) \gg \mathcal{O}\left(\ell_{\rm P}\log\left(\frac{R_0(u)}{\ell_{\rm P}}\right)\right). \tag{30}$$

Even for a shell as heavy as 10^{10} solar mass, ΔL only needs to be greater than 110 times the Planck length for the approximation above. Therefore, in a low-energy effective theory applicable only to energies well below 10^{17} GeV, such a pseudo thin shell is indistinguishable from an ideal thin shell.

To calculate Hawking radiation, we take the time derivative of equation (28):

$$\dot{\psi}_0(u) \simeq -\frac{R_0(u)\dot{R}_0(u) - R_i(u)\dot{R}_i(u)}{2\sigma}. \tag{31}$$

Assuming that $R_i(u)$ is falling at the speed of light,

$$\begin{aligned}\dot{R}_i(u) &= -\frac{1}{2}\mathrm{e}^{\psi(u,R_i(u))}\frac{R_i(u) - a_i(u)}{R_i(u)}\\ &\simeq -\frac{1}{2}\mathrm{e}^{-\frac{R_0^2(u)-R_i^2(u)}{4\sigma}}\frac{R_i(u) - a_i(u)}{R_i(u)}.\end{aligned} \tag{32}$$

The huge redshift factor above

$$\mathrm{e}^{-\frac{R_0^2(u)-R_i^2(u)}{4\sigma}} \simeq \mathrm{e}^{-\frac{R_0(u)(R_0(u)-R_i(u))}{2\sigma}} \gg \frac{\sigma}{R_i^2(u)} \tag{33}$$

implies that the 2nd term in equation (31) is much smaller than the 1st term. Hence,

$$\dot{\psi}_0(u) \simeq -\frac{R_0(u)\dot{R}_0(u)}{2\sigma} \simeq \frac{1}{2a_0(u)}, \tag{34}$$

which is the same as equation (42) for a slope-1 shell in section 4, but differs significantly from the ideal thin shell in section 3.1.2[6]. As a result, this thin shell of a finite thickness will evaporate completely, rather than approaching a classical black hole like the ideal thin shell.

It is an interesting coincidence that the Hawking radiation of the pseudo thin shell (with its back-reaction included in the calculation) happen to agree with that of the ideal thin shell when the back-reaction is ignored, while they disagree when the back-reaction is turned on. This observation suggests that, despite its sensitivity to modifications at a length scale slightly larger than the Planck scale, e.g. $100\ell_{\rm P}$ for a shell of 10^{10} solar mass, there is still some robustness in the Hawking radiation of the conventional model of black holes.

3.3. Analogy with electromagnetism

The pseudo thin shells considered above imply that the equations governing the Hawking radiation (7) is too sensitive to Planck-scale details so that the notion of ideal thin shells is inappropriate for discussions in the context of low-energy effective theories.

[6] Equation (34) differs significantly from the ideal thin shell (with back-reaction from Hawking radiation) in section 3.1.2 which has $\dot{\psi}_0 \to 0$. It also differs by an overall sign from the conventional result (15) which ignores the back-reaction of Hawking radiation.

Similar issues have been discussed in other branches of physics. It is not uncommon for low-energy effective theories to involve higher-derivative terms. Typically, such higher-derivative terms lead to various pathologies. A well known simple example can be found in the textbook on classical electromagnetism [38]. According to the Abraham–Lorentz formula, the back-reaction force of the electromagnetic radiation by a point charge is proportional to the 2nd time-derivative of the velocity of the charge. Any solution of a point-charge is then either a runaway solution (accelerating indefinitely to infinite velocity even after all external forces are removed—instability), or it suffers pre-acceleration (acceleration before external forces are applied—a violation of causality). The proper way to deal with this issue is, of course, to keep in mind that, strictly speaking, it is unreasonable to claim a charge to be point-like in a low-energy effective theory. The equation of motion should be solved for a charge with finite size and finite density, and the point charge limit, up to the cut-off scale, should be taken after solving the equation. As long as all charge distributions have a sufficiently smooth profile, these problems can be ignored.

In the light of this analogy, a pseudo thin shell satisfying the inequality (30)) is a valid thin-shell configuration in the low-energy effective theory, while the ideal thin shell is not.

It is well known that the Abraham–Lorentz formula is still applicable to point charges in perturbative calculations. At the lowest-order approximation, a point charge is assumed to move without back-reaction. The first-order correction to the point-charge trajectory due to back-reaction can then be calculated, and it provides a good approximation whenever the radiation is sufficiently weak.

In general, in a low-energy effective theory, one can consider a derivative expansion, which would be truncated at a certain order of the expansion. Assuming that higher-derivative terms are less important, the physical result should not be dramatically changed when the order of the truncation is slightly changed. However, higher-derivative terms always introduce new solutions and new instabilities. An approach to deal with the higher-derivative terms in a low-energy effective theory was suggested by Yang and Feldman [39], which was later extended to a general formulation in [40]. Following this prescription, one can include the effect of higher-derivative terms order by order without introducing unphysical solutions. In the rest of this paper, we adopt this approach to take care of the higher derivatives in the Schwarzian derivative in equation (7).

Notice that, the ideal thin shell without back-reaction from Hawking radiation and the pseudo thin shell produces the same formula

$$\frac{\mathrm{d}a}{\mathrm{d}u} \simeq -\frac{\kappa\mathcal{N}}{48\pi a^2} \tag{35}$$

for Hawking radiation. This is compatible with our analogy with point charges in classical electromagnetism. We will, therefore, take this formula (35) as the lowest-order approximation for the Hawking radiation from pseudo thin shells. Corrections from higher-order terms in the Schwarzian derivative can then be added iteratively order by order. We will compute the first-order correction and check that it is small in our simulation.

4. Slope-1 shell

In this section, we review the smooth configuration of the collapsing matter proposed in [1]:

$$a(u,r)=\begin{cases} a_0(u)\equiv R_0(u)-\frac{2\sigma}{R_0(u)}, & r>R_0(u),\\ r-\frac{2\sigma}{r}, & R_0(u)>r>R_1(u),\\ <r-\frac{2\sigma}{r}, & r<R_1(u), \end{cases} \tag{36}$$

where σ is given by equation (27). We assume that $R_0(u)-R_1(u)$ is of a macroscopic value much larger than $\frac{\sigma}{a}$. The matter at r has approached the Schwarzschild radius $a(u,r)$ for the total mass inside r, and the slope of $a(u,r)$ as a function of r is approximately equal to 1 within the range of $r\in(R_1(u),R_0(u))$. The functional form of $a(u,r)$ within the inner part of the shell for $r<R_1(u)$ will turn out to be irrelevant due to the huge redshift factor.

The slope of the $a-r$ curve is approximately 1 for this profile, so we will refer to it as a *slope-1 shell*. The slope-1 shell is interesting because it is an asymptotic solution compatible with the following assumptions: (1) all layers of the collapsing matter are close to their Schwarzschild radii, and (2) the decay rate due to Hawking radiation is given by equation (17). We also show in the appendix that slope-1 configurations of an arbitrary thickness are unique as asymptotic states under certain assumptions.

The outer radius $R_0(u)$ satisfies equation (13) as it falls at the speed of light. When the shell is sufficiently close to the Schwarzschild radius, it can be approximated as

$$R_0(u)=a_0(u)-2R_0(u)\frac{\mathrm{d}R_0(u)}{\mathrm{d}u}\simeq a_0(u)-2a_0(u)\frac{\mathrm{d}a_0}{\mathrm{d}u}\,. \tag{37}$$

Combining it with equation (17), we see that [1]

$$R_0(u)\simeq a_0(u)+\frac{2\sigma}{a_0(u)}. \tag{38}$$

The inverse of this relation is

$$a_0(u)\simeq R_0(u)-\frac{2\sigma}{R_0(u)}. \tag{39}$$

For spherically symmetric configurations, we can decompose the collapsing matter into infinitely many infinitesimal collapsing layers labeled by a number n. The total mass enclosed in each shell of radius R_n defines the Schwarzschild radius a_n associated to that shell. (The geometry of the infinitesimal gap between the nth layer and the $(n+1)$st layer is thus determined by a_n.) we can, therefore, apply the same argument to every layer below the surface, to claim that eventually

$$R_n(u)\simeq a_n(u)+\frac{2\sigma}{a_n(u)}, \tag{40}$$

and hence equation (36) is motivated. This was why the slope-1 configuration was referred to as the 'asymptotic black hole' in [7].

For this smooth configuration (36), equation (5) implies that

$$\psi_0(u)\simeq-\frac{R_0^2(u)}{4\sigma}, \tag{41}$$

so that

$$\dot{\psi}_0(u)\simeq-\frac{R_0(u)\dot{R}_0(u)}{2\sigma}\simeq-\frac{a_0(u)\dot{a}_0(u)}{2\sigma}\simeq\frac{1}{2a_0(u)}. \tag{42}$$

Notice that this differs from the conventional result (15) for the ideal thin shell without back-reaction by a sign, but the Hawking radiation is the same at the leading order! It is very different from the case of the ideal thin shell when the back-reaction of Hawking radiation is taken into consideration.

It was proposed in [7] that, from the viewpoints of distant observers, the slope-1 configuration is expected to appear as an asymptotic configuration for generic initial states of the collapsing matter. On the other hand, it was also noted there that, as the surface of the collapsing shell gets very close to the Schwarzschild radius (i.e. when equation (38) is satisfied), everything below a short depth under the surface is essentially frozen. It is, therefore, possible that the collapsing matter demonstrates a different asymptotic profile. One of the main results of this paper is to show that, even though the slope-1 configuration is indeed an asymptotic state, there exists another asymptotic state.

5. Asymptotic states

The rest of the paper is focused on the question 'What are the asymptotic states of gravitational collapses?' First, in section 5.1, we consider the collapsing layers in the static Schwarzschild background. The back-reaction of Hawking radiation is ignored, and the geometry between the collapsing layers is given by the static Schwarzschild background. In section 5.2, we describe our result about how things are different when the back-reaction is turned on.

5.1. Without back-reaction of Hawking radiation

For a static Schwarzschild background, each layer in the collapsing matter approaches its event horizon. If the initial profile has a slope $\mathrm{d}a/\mathrm{d}r$ much smaller than 1, the inner layers approach their Schwarzschild radii earlier, and the outer layers to theirs later. The inner layers do not impose redshift factors to slow down the collapse of outer layers for a distant observer. Therefore, in the end, for distant observers, all the layers are quite close to their Schwarzschild radii and the profile of the whole collapsing matter is frozen. Such configurations approach states with slopes $\mathrm{d}a/\mathrm{d}r$ approximately equal to 1, although in detail they are in general different from the slope-1 state described in section 4. The attractor states have slope 1 for initial states with sufficiently small slopes $\mathrm{d}a/\mathrm{d}r$.

If, however, the initial state has a slope $\mathrm{d}a/\mathrm{d}r$ larger than 1, the outer layers approach their Schwarzschild radii earlier, and they impose a large redshift factor on the inner layers from the viewpoint of a distant observer. With the inner layers frozen by the large redshift factor, the profile of the inner layers remains essentially the same as the initial state. There is no unique asymptotic profile in this case.

This picture will be modified by turning on the back-reaction of Hawking radiation.

5.2. Back-reaction of Hawking radiation

When the back-reaction of Hawking radiation is taken into consideration, the situation is slightly changed. The geometries between the layers are given by the outgoing Vaidya metric, whose Schwarzschild radii have time dependence and are decreasing due to the effect of Hawking radiation. The profile of the energy distribution is affected by the time dependence of the Schwarzschild radii between the layers.

For a profile with $\mathrm{d}a/\mathrm{d}r \ll 1$, the inner layers would get close to their Schwarzschild radii before the outer layers do theirs, so the inner layers evaporate first. As in the case without the

back-reaction, the outer layers are never frozen, so they keep falling in until they also approach their Schwarzschild radii. Eventually, all layers are close to their Schwarzschild radii, and this is the slope-1 configuration (section 4). It looks approximately the same as the asymptotic state without the back-reaction in section 5.1. The effect of the back-reaction gives no significant modification before the layers approach the slope-1 configuration. The layers are still moving inward even after it becomes the slope-1 configuration since the Schwarzschild radii are decreasing. However, the profile remains the same.

On the other hand, for an initial state with a large slope $\mathrm{d}a/\mathrm{d}r \gg 1$, the outer layers reach close to their Schwarzschild radii $a(u, r)$ before the inner layers do. The inner layers are frozen by the $1/(r - a)$ contribution of the outer layers due to the redshift factor (4), and the outer layers evaporate first. As the outer layers are evaporating, the thickness of an outer layer close to its Schwarzschild radius $a(u, r)$ reduces over time until it is barely thick enough to keep the inner shells frozen. As outer layers evaporate away, inner layers are thawed and start falling close to their Schwarzschild radii. After the evaporation of the outer layers, the outermost part of the inner layers plays the role of the outer layers. If the profile of the inner layers also has a large slope $\mathrm{d}a/\mathrm{d}r \gg 1$, the same process to the above is repeated. Thus, the thickness of the whole shell decreases over time. Although the inner part of the collapsing matter deep under its surface still has an arbitrary profile depending on the initial condition, the part close to the surface approaches a thin shell. The thin shells can thus be viewed as another class of asymptotic states. The back-reaction of Hawking radiation plays an important role in this mechanism. This result is quite different from the case without the back-reaction.

6. Numerical simulation

In this section, through numerical methods, we investigate the dynamical process leading to the asymptotic states described in the previous section. As it was explained in section 3, we shall not consider ideal thin shells and the higher-derivative terms in the Hawking radiation should be treated in a way suitable for the low-energy effective theory.

6.1. Numerical methods

In numerical simulation, we discretized the continuous matter distribution as a set of collapsing thin shells labeled by a number $n = 1, 2, \cdots, N$ from the innermost shell ($n = 1$) to the outermost shell ($n = N$). Each shell has a radius R_n, and the total mass M_n enclosed in the shell defines the Schwarzschild radius $a_n = 2GM_n$ associated with the shell. The metric between the nth shell and the $(n + 1)$st shell is given by the outgoing Vaidya metric and determined by the Schwarzschild radius a_n.

As it was explained in section 3.3, we adopt the perturbative approach in which each layer of the thin shell evaporates according to equation (35), to avoid unphysical dependence on Planck-scale structures. Hence, we assume that for the nth layer, at the leading order

$$\frac{\mathrm{d}a_n}{\mathrm{d}u_n} \simeq -\frac{\sigma}{a_n^2} \qquad \left(\sigma \equiv \frac{\kappa\mathcal{N}}{48\pi}\right), \tag{43}$$

where u_n is the outgoing light-cone coordinate for the segment between the nth and the $(n + 1)$ st shell. This assumption is iterated back into the Schwarzian derivative $\{u_n, U\}$ for the first-order correction.

Schematically, the first-order correction is calculated in the following way. The Schwarzian derivative introduces first and second-order derivatives of a_n into the decay rate equation of a_n as

$$\frac{\mathrm{d}a_n}{\mathrm{d}u_n} = f\left(a_n, \frac{\mathrm{d}a_n}{\mathrm{d}u_n}, \frac{\mathrm{d}^2 a_n}{\mathrm{d}u_n^2}, R_n\right), \tag{44}$$

through a certain function f. In general, there could be dependence on the first and second derivatives of R_n in the function f, but they can be traded for zeroth and first derivatives of a_n through the evolution equation of R_n

$$\frac{\mathrm{d}R_n}{\mathrm{d}u_n} = -\frac{1}{2}\left(1 - \frac{a_n}{R_n}\right), \tag{45}$$

respectively. By using this equation repeatedly, the derivatives of R_n can be removed from the expression of f, and therefore, f in (44) does not depend on the derivatives of R_n. Thus the decay rate equation (44) contains only the derivatives of a_n.

As we explained in section 3.3, to avoid the pathologies introduced by higher derivatives, we will solve the equation by the perturbative method. We first take the conventional formula (43) as the zeroth-order approximation for $\frac{\mathrm{d}a_n}{\mathrm{d}u_n}$. As a result,

$$\frac{\mathrm{d}^2 a_n}{\mathrm{d}u_n^2} \simeq \frac{-2\sigma^2}{a_n^5}, \tag{46}$$

so that $\frac{\mathrm{d}a_n}{\mathrm{d}u_n}$ and $\frac{\mathrm{d}^2 a_n}{\mathrm{d}u_n^2}$ on the right-hand side of equation (44) can be replaced by functions of a_n and R_n, without their time derivatives at all. This way, we get a first-order differential equation for a_n. That is, $\frac{\mathrm{d}a_n}{\mathrm{d}u_n}$ is given by a function of a_n and R_n. (It is straightforward to derive this lengthy expression so we will not present it here.) In general, one can do this iteratively to get higher-order corrections to obtain a more accurate approximation. We will check that the first-order correction is small, and ignore higher-order corrections.

To study the astrophysical black holes, we need to consider a sufficiently large mass. To study such a large mass, a huge number of layers are necessary. However, the simulation of a lot of layers is computationally expensive. Here, we are interested in the asymptotic states of the collapsing layers, in particular, whether they approach the slope-1 state or evaporate from the outer layers. To see this, it is sufficient to study the outer shells. To save computer time in our simulation, we sometimes include a massive core at the center that also evaporates according to the conventional formula (43). This way we can efficiently describe a configuration with a large mass, while we focus on the behaviors of the outer shells, and see if they evaporate first. Note that the inner core is essentially frozen because of the strong redshift factor due to the outer shells when the outer shells are close to their Schwarzschild radii, so we do not expect the replacement of many inner shells by a massive core to make much difference to the behavior of the outer shells. To verify this assumption, one can compare the dynamics of the outer n layers of a system of $N + n$ layers of collapsing shells, versus the dynamics of n layers in a second system, in which a massive core replaces the N shells of the first system. One can check that the dynamics of the n shells in both systems agree. Furthermore, one can check that the geometry outside all the shells agrees with that of a single massive core of the same total mass. Hence the assumption can be justified by induction.

6.2. Numerical results

Now, we study the time evolution of collapsing layers, taking the back-reaction of Hawking radiation into account. Unless otherwise specified, the time evolution R_n and a_n will be presented as functions of the light-like coordinate $u = u_0$ outside all shells.

We assume that there is no horizon in the initial state, that is, no shell is inside its Schwarzschild radius,

$$R_n(u_{\rm init}) > a_n(u_{\rm init}) \qquad \forall n \tag{47}$$

at the initial time $u = u_{\rm init}$. $R_n(u)$ decreases as the nth shell collapses. Its associated Schwarzschild radius $a_n(u)$ slowly decreases due to Hawking radiation when $R_n(u)$ gets close to $a_n(u)$.

The profile of a collapsing matter distribution at any given time u is given by the plot of a_n versus R_n for that u. While the profile (the $a - r$ graph) of the initial configuration is arbitrary except that it must be a monotonically increasing relation, we shall focus on linear profiles with various slopes. Once they are understood, it is straightforward to generalize the knowledge to a generic profile by decomposing the profile into many small segments which are approximated by linear relations between a and r.

With the assumption that all layers n are falling at the speed of light, the radius R_n satisfies the equation

$$\frac{{\rm d}R_n(u)}{{\rm d}u} = -\frac{1}{2}{\rm e}^{\psi_n}\frac{R_n - a_n}{R_n}. \tag{48}$$

This assumption also ensures that the shells do not cross each other. When the collapsing matter is still far away from its Schwarzschild radius, at large distances where the spacetime is nearly flat, the $a - r$ profile remains roughly unchanged as it shifts along the r-axis over time. We shall, therefore, focus on the initial states in which at least a part of the $a - r$ profile is very close to the $a = r$ line. That is, some of the layers have already approached their Schwarzschild radius | $R_n \simeq a_n$ for at least some values of n.

When the radius R_n of a layer n is close to its Schwarzschild radius a_n, the decreasing rate in R_n slows down. If the initial slope is smaller than 1, the innermost layers get close to the curve $a = r$ first, and then, the slope $\partial a/\partial r$ increases over time. If the initial slope is larger than 1, the outermost layers approach $a = r$ first. In this case, the inner layers also slow down because of the redshift factor due to the outer shells. Therefore, the slope does not decrease. See figures 1–4 for the profiles at each moment of the collapse. It should be noted that, for a large initial slope of the profile, the effect of the redshift factor appears because the time evolution is measured by using the time coordinate outside all shells. Although the collapse does not slow down for the local observer at the inner layers, it slows down for the observer outside the collapsing matters.

Despite the tendency of increasing the slope $\partial a/\partial r$ over time, once a layer is very close to the $a = r$ line, it can only move diagonally along the $a = r$ line (more precisely, a curve along which $r \simeq a + \frac{2\sigma}{a}$). Our simulation shows that, for initial configurations with slopes $\partial a/\partial r \ll 1$, the slope only approaches 1 in the end, while configurations with initial slopes $\partial a/\partial r \gg 1$, the slope approaches infinity, which implies that the collapsing layers approach a thin shell.

To conclude, there are two distinct classes of asymptotic states of black holes. The first class approaches the slope-1 configuration, for initial profiles with a small slope. The second class approaches thin-shell configurations for initial profiles with large slopes. The criterion

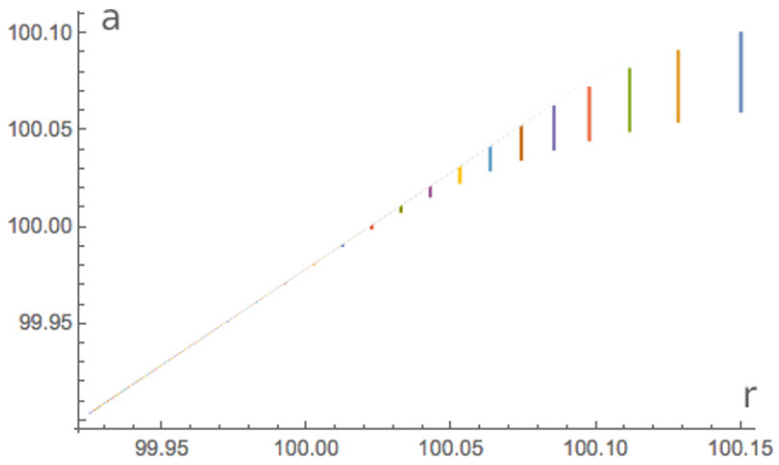

Figure 1. $a - r$ graph for $\frac{\partial a}{\partial r} = \infty$. The profile of the collapsing sphere is shown at different instants of u. The initial state with $\frac{\partial a}{\partial r} = \infty$ is the first vertical line on the right. The profile gets shorter as it moves to the left due to evaporation. The slope remains infinite throughout the dynamical process.

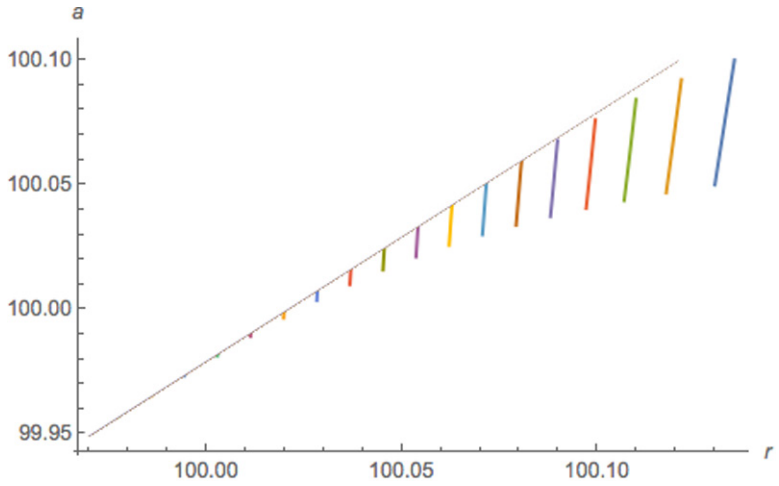

Figure 2. $a - r$ graph for $\frac{\partial a}{\partial r} = 10$. The profile of the collapsing sphere is shown at different instants of u. The initial state with $\frac{\partial a}{\partial r} = 10$ is the first vertical line on the right. The profile gets shorter as it moves to the left due to evaporation. The slope approaches infinite in the dynamical process.

deciding whether an initial configuration evolves towards one class or another is whether the slope of the initial profile $\mathrm{d}a/\mathrm{d}r$ is much smaller than 1 or much larger than 1.

We considered only the profiles with constant slopes so far. It is straightforward to study more generic profiles. For example, if the slope for inner layers is large but that for outer layers is small, the middle layers will approach the line of $a = r$ first. The inner layers will be frozen and moving inward without changing the slope, while the outer layers will asymptote to the slope-1 configuration.

Recall that the volume density of matter is defined as

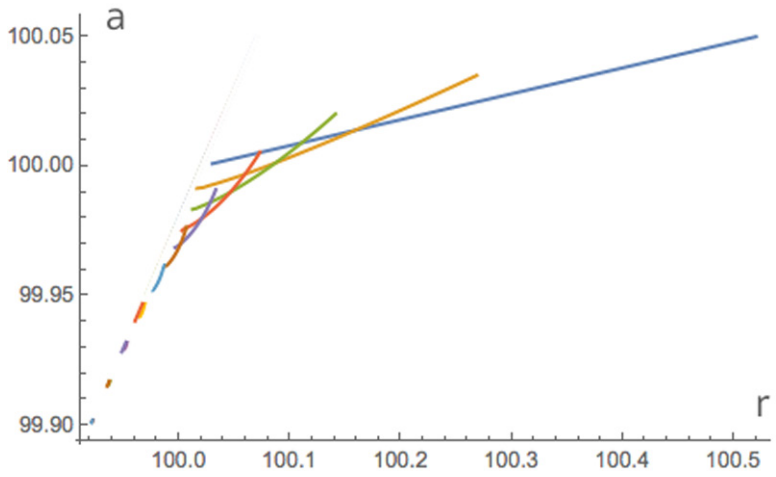

Figure 3. $a-r$ graph for $\frac{\partial a}{\partial r}=0.1$. The profile of the collapsing sphere is shown at different instants of u. The initial state with $\frac{\partial a}{\partial r}=0.1$ is the first straight line (blue). The profile gets shorter and the slope becomes larger as it moves to the left. Eventually, the slope approaches 1.

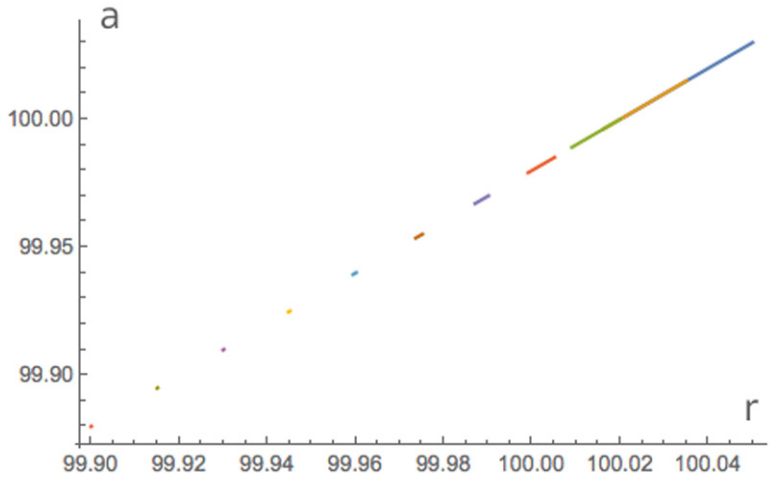

Figure 4. $a-r$ graph for $\frac{\partial a}{\partial r}=1$. The profile of the collapsing sphere is shown at different instants of u. The initial state with $\frac{\partial a}{\partial r}=1$ is the diagonal line in blue, partially overlapping with the profile at later times. The profile gets shorter and the slope remains approximately equal to 1.

$$\frac{\mathrm{d}m}{\mathrm{dvol}}=\frac{1}{8\pi G_N r^2}\frac{\mathrm{d}a}{\mathrm{d}r}, \tag{49}$$

so the critical volume density ρ_c (around the Schwarzschild radius) corresponding to $\mathrm{d}a/\mathrm{d}r=1$ is

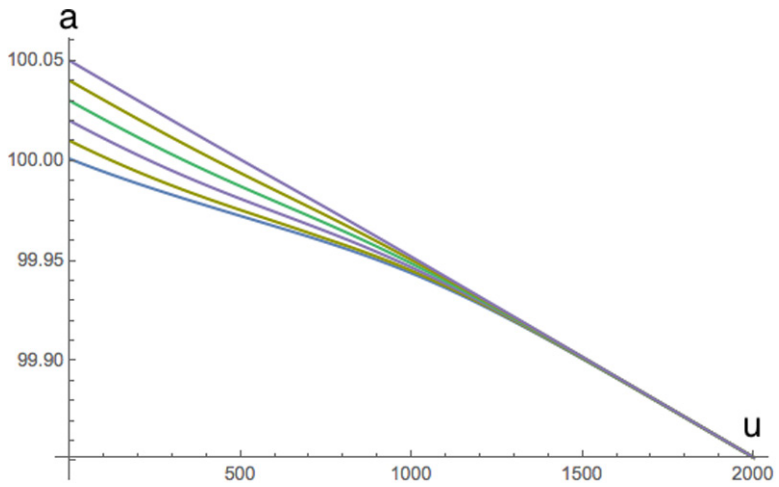

Figure 5. $a(u)$ for $\mathrm{d}a/\mathrm{d}r = 0.1$. The values a_n for all layers are shown as functions of time u. The values of a_n do not start at 0 because there is a massive core at the center. The innermost layers evaporate first, so in the diagram, they merge with other layers initially on top of them. At larger u, the outermost layers evaporate and appear to merge with other layers initially under them.

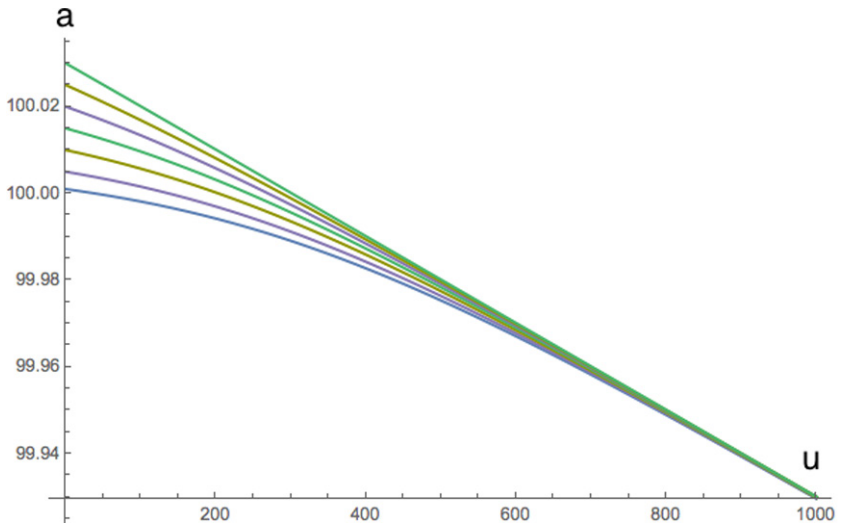

Figure 6. $a(u)$ for $\mathrm{d}a/\mathrm{d}r = 1$. The values a_n for all layers are shown as functions of time u. The values of a_n do not start at 0 because there is a massive core at the center. The outermost layers evaporate first so they appear to merge with other layers initially under them.

$$\rho_c \equiv \frac{1}{4\pi r^2}\frac{\partial M}{\partial r}\bigg|_{\text{critical}} \simeq \frac{1}{8\pi G_N a^2} = \frac{1}{\kappa a^2}, \tag{50}$$

where we have used $a = 2G_N M$. This corresponds to a volume density of order $\mathcal{O}(1/a^4)$ at a distance of order $\mathcal{O}(a)$ away from the horizon. It is of the same order of magnitude as the

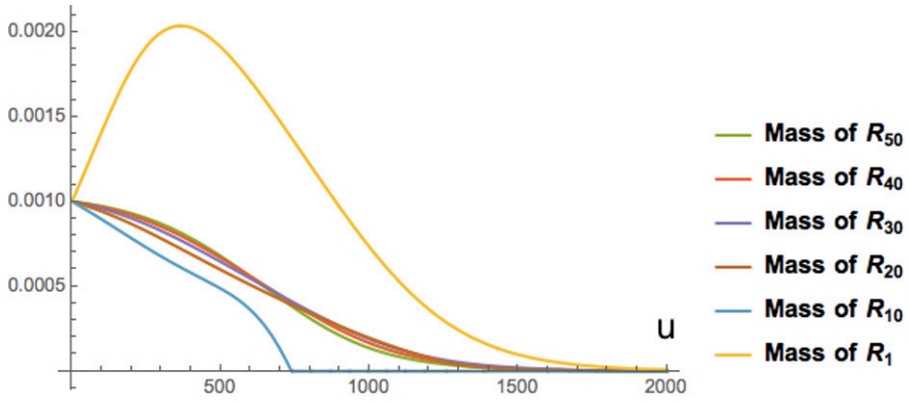

Figure 7. $m(u)$ for $\partial a/\partial r = 0.1$. The masses of some of the layers are shown as functions of time u. It is clear that, generically, inner layers evaporate faster in the beginning, while outer layers evaporate faster at a later time. There is roughly a point of intersection of the curves when they have evaporated the same percentage of their masses. The mass of the first layer R_1 outside the massive core appears to be anomalous as it initially increases with time. This is because the outgoing energy due to the evaporation of the massive core is temporarily counted as its energy. This is merely an artifact of our choice of the configuration.

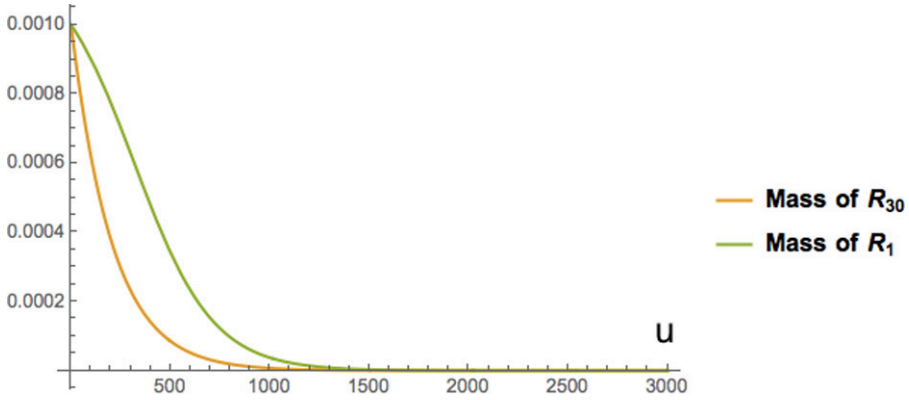

Figure 8. $m(u)$ for $\partial a/\partial r = 1$. The masses of some of the layers are shown as functions of time u. The situation is simple in this case: outer layers evaporate faster than inner layers at all times.

Hawking radiation. In fact, the ingoing energy of the collapsing matters balances with that of Hawking radiation in the special case of the slope-1 configuration which is studied in [1]. Hence, we expect the ingoing energy flux of density higher (lower) than Hawking radiation to resemble the thin shell (slope-1 configuration) as it approaches the horizon.

Even for a black hole as small as a solar mass, its Hawking radiation is much weaker than the current cosmic microwave background radiation. Hence all existing black holes are expected to have a surface layer resembling the thin shell configuration. That is, the slope $\mathrm{d}a/\mathrm{d}r$ is very large at the surface of the black hole.

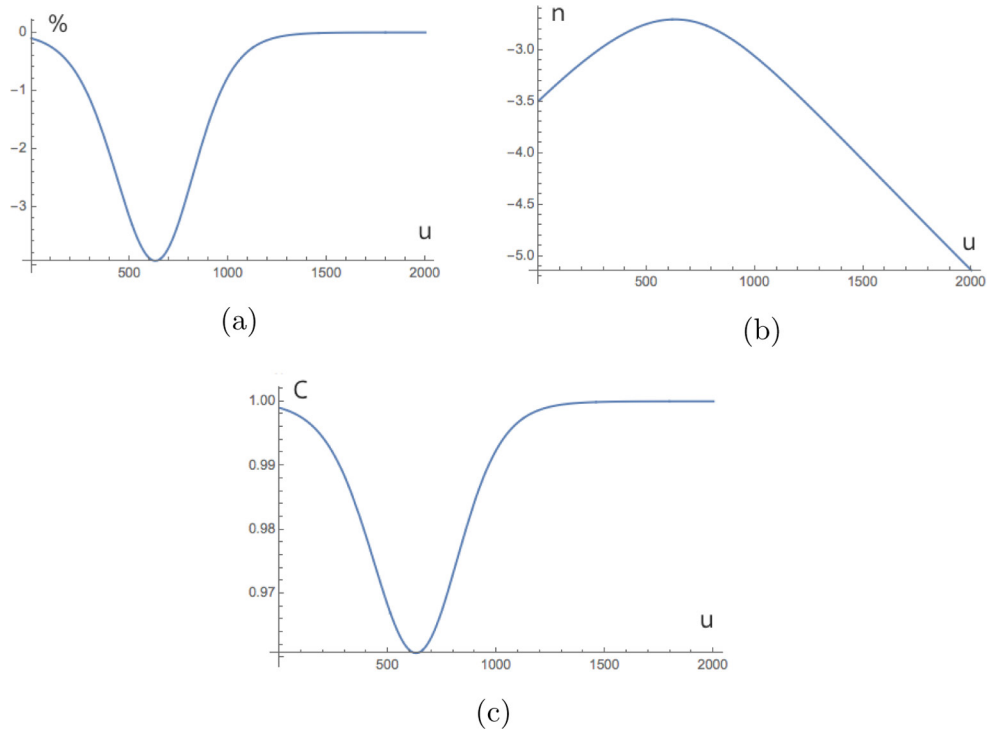

Figure 9. 1st-order correction in Hawking radiation for $\frac{\mathrm{d}a}{\mathrm{d}r} = 0.1$. (a) The first-order correction $\Delta\left(\frac{\mathrm{d}a}{\mathrm{d}u}\right)$ as percentage of the 0th-order expression of $\frac{\mathrm{d}a}{\mathrm{d}u}$. (b) Modeling the dependence of the first-order correction $\Delta\left(\frac{\mathrm{d}a}{\mathrm{d}u}\right)$ by power law $\Delta\left(\frac{\mathrm{d}a}{\mathrm{d}u}\right) = Aa^n$ for some constant A. (c) Modeling the first-order correction by the coefficient C in $\Delta\left(\frac{\mathrm{d}a}{\mathrm{d}u}\right) = \frac{(1-C)\sigma}{a^2}$.

6.3. Stages of evaporation

In the KMY model, it was found [1] that, for the ideal slop-1 shells, the collapsing shells are moving inward as they lose the energy by Hawking radiation. It is also argued [4] that the evaporation of the collapsing shells, in most cases, happens in the same fashion as peeling an onion—layer by layer from the outside. The reason is that the inner shells are frozen due to the huge redshift factor.

Here we would like to ask in general, when would the evaporation start from the layers on the outside or the inside. To see this, we calculate the time evolution of the Schwarzschild radii for each shell, as functions of u. We find that the evaporation process is a competition between the suppression due to a large redshift factor and the enhancement of evaporation due to the short separation of a layer from its Schwarzschild radius a. The details are described in the following.

6.3.1. Small-slope configurations. For the profile of a collapsing matter with a very small slope ($\mathrm{d}a/\mathrm{d}r \ll 1$), the innermost shell approaches its Schwarzschild radius before the other shells and starts to evaporate first. As more and more layers approach their Schwarzschild

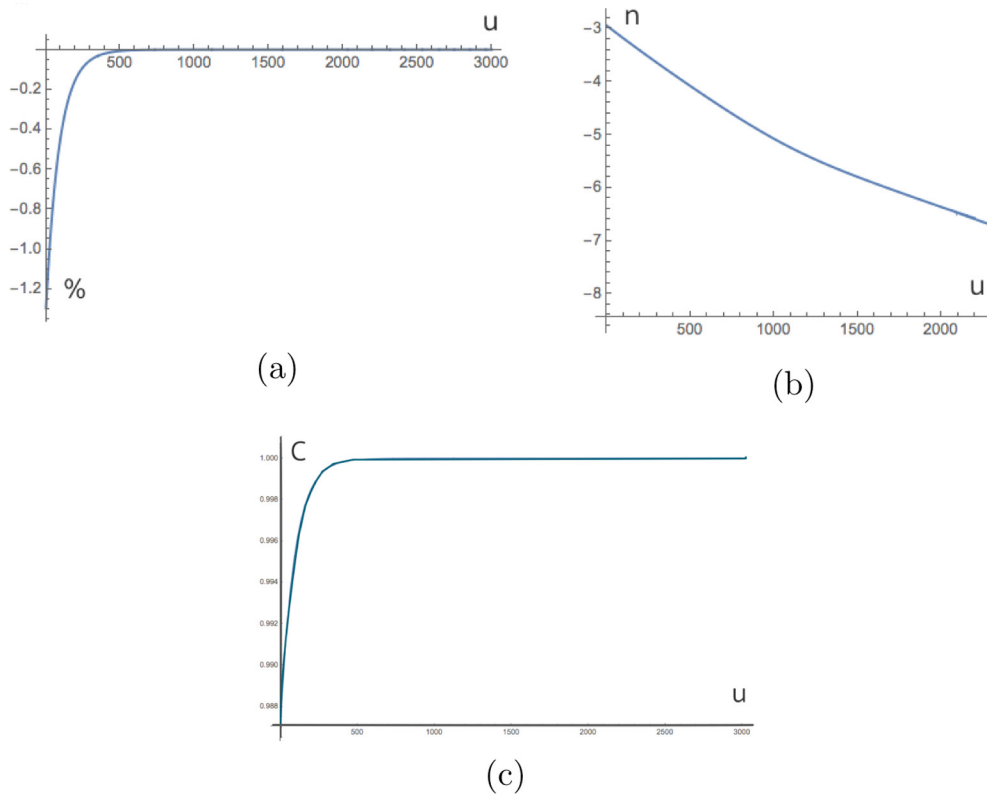

Figure 10. 1st-order correction in Hawking radiation for $\frac{da}{dr} = 1$. (a) The first-order correction $\Delta\left(\frac{da}{du}\right)$ as percentage of the 0th-order expression of $\frac{da}{du}$. (b) Modeling the dependence of the first-order correction $\Delta\left(\frac{da}{du}\right)$ by power law $\Delta\left(\frac{da}{du}\right) = Aa^n$ for some constant A. (c) Modeling the first-order correction by the coefficient C in $\Delta\left(\frac{da}{du}\right) = \frac{(1-C)\sigma}{a^2}$.

radii, a layer that is already close to its Schwarzschild radii will stay locked at a separation $R_n - a_n \simeq 2\sigma/a_n$ until it is evaporated.

As the outer layers approach their Schwarzschild radii, the redshift factor becomes large for the remaining inner layers, so that the radiation from the remaining inner layers is suppressed. The outer layers are then evaporated before them.

Therefore, for a profile with a tiny slope, its evaporation can be very roughly decomposed into two stages. In the first stage, the inner layers evaporate first, and the outer layers are still far from their Schwarzschild radii. In the 2nd stage[7], after it has turned into a slope-1 configuration, the outer layers get close to their Schwarzschild radii and start to evaporate, and the inner layers surviving the first stage are frozen until outer layers are evaporated. The configuration of the collapsing matter is now in agreement with the slope-1 shell.

This process is shown in figure 5. The plot consists of many curves of the Schwarzschild radii for each shell. A layer completely evaporates when the curve merges with the next curve—its Schwarzschild radius becomes the same as that of the inner layer. In comparison,

[7] This is the stage of onion peeling described in the KMY model.

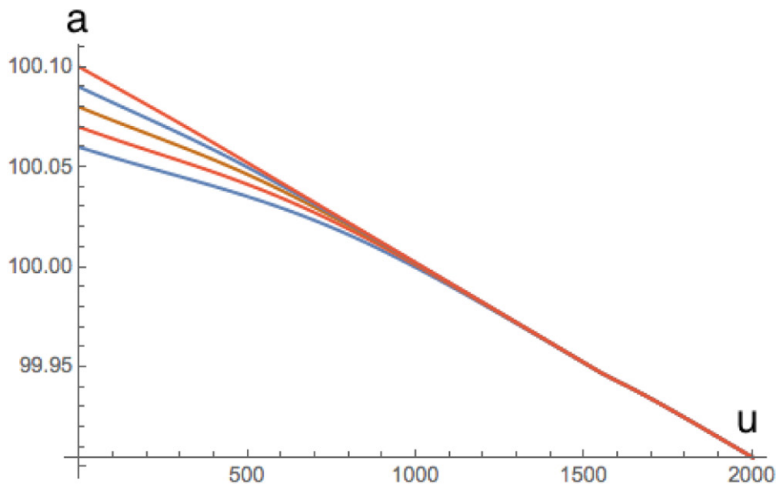

Figure 11. $a(u)$ for $\partial a/\partial r = \infty$. The values a_n for all layers are shown as functions of time u. The values of a_n do not start at 0 because there is a massive core at the center. The outermost layers evaporate first, so in the diagram, they appear to merge with other layers initially below them.

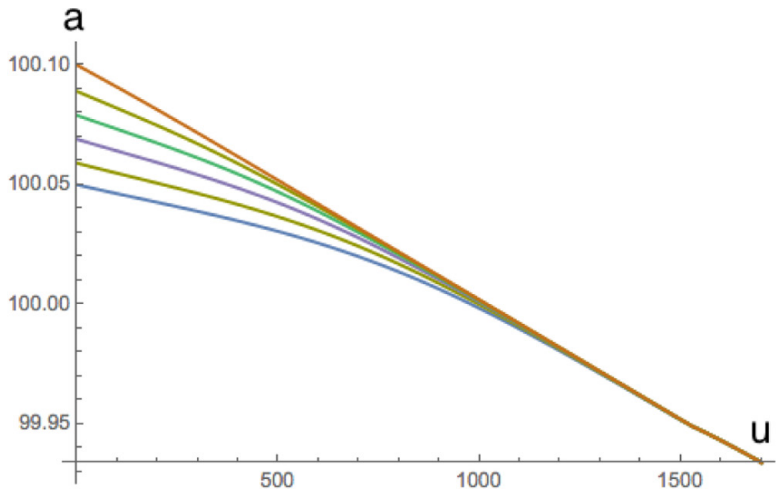

Figure 12. $a(u)$ for $\partial a/\partial r = 10$. This diagram is essentially the same as figure 11.

the process for $\partial a/\partial r \simeq 1$ is shown in figure 6, for which the outer layers are evaporated first, resembling the late stage of figure 5.

By the analogy with the radiation of point charges in classical electromagnetism in section 3.3, the gravitational collapse with Hawking radiation in our formulation should be free of pathological instabilities. Indeed, in all of our numerical simulation, the system under study always approaches one of the asymptotic states. Nevertheless, we study in more detail the transition process towards the asymptotic states.

The time-dependence of the masses of different shells are plotted in figures 7 and 8 for $\partial a/\partial r = 0.1$ and $\partial a/\partial r = 1$, respectively. In both cases, after a short time with non-uniform behavior, the collapsing shells approach the asymptotic states.

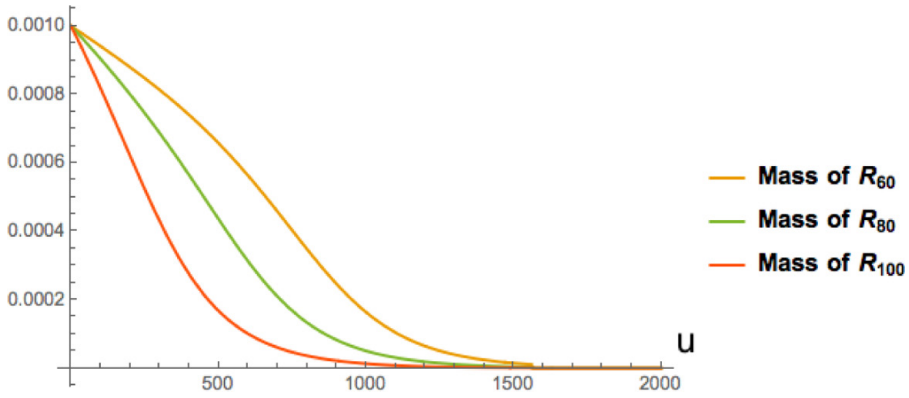

Figure 13. $m(u)$ for $\partial a/\partial r = \infty$. The masses of some of the layers are shown as functions of time u. Generically, outer layers evaporate faster.

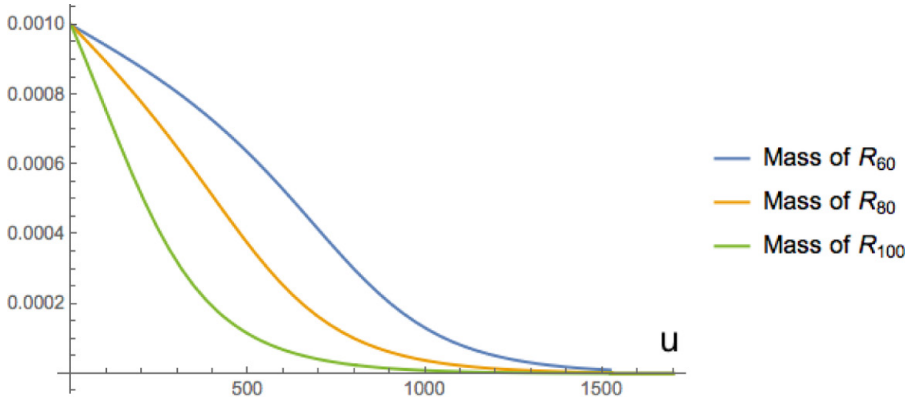

Figure 14. $m(u)$ for $\partial a/\partial r = 10$. This diagram is essentially the same as figure 13.

For both $\frac{da}{dr}$ equal to 0.1 and 1, the first-order correction to the 0th-order Hawking radiation is relatively small. We analyzed this deviation in three different ways: (1) the percentage of correction with respect to the 0th-order amplitude: $\Delta\left(\frac{da}{du}\right)/\frac{da^{(0)}}{du}$, (2) how the correction $\Delta\left(\frac{da}{du}\right)$ scales with a during the collapsing process, and (3) If we use the formula $\frac{da}{du} = -C(u)\sigma/a^2$ to model the Hawking radiation, how is the coefficient $C(u)$ changing with time. In all analyses, we find the first-order correction to Hawking radiation sufficiently small to justify our perturbative interpretation of the Schwarzian derivative. See figure 9 for $\frac{da}{dr} = 0.1$ and figure 10 for $\frac{da}{dr} = 1$.

6.3.2. Large-slope configurations. For a collapsing profile with a large slope ($da/dr \gg 1$), the outer layers reach close to their Schwarzschild radii earlier than the inner layers. Hence the inner layers are frozen until outer layers are evaporated.

Whenever the outer layers are very close to their Schwarzschild radii, the inner layers are frozen by the large redshift factor, and the radiation of the inner layers can be ignored (in terms of the time coordinate u) regardless of whether the inner layers are close to their Schwarzschild radii. Therefore, for a collapsing ball with an outer surface that has been evaporating for a long time, it is evaporating from the outer layers in most cases. See figures 11 and 12.

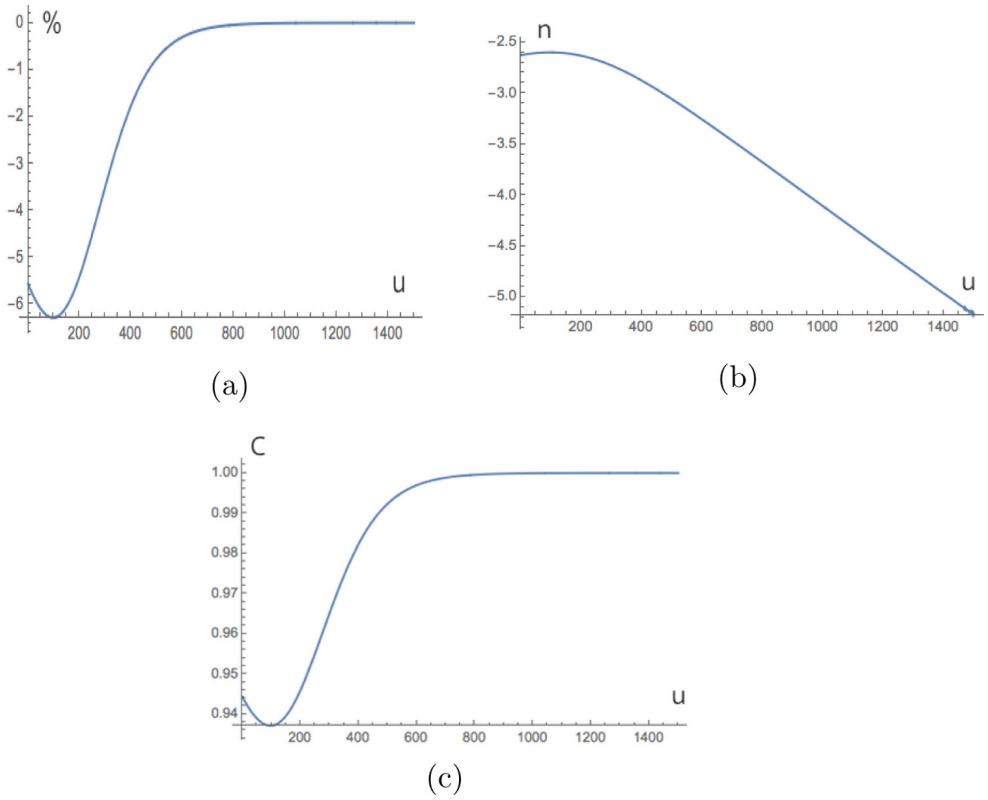

Figure 15. 1st-order correction in Hawking radiation for $\frac{\mathrm{d}a}{\mathrm{d}r} = \infty$. (a) The first-order correction $\Delta\left(\frac{\mathrm{d}a}{\mathrm{d}u}\right)$ as percentage of the 0th-order expression of $\frac{\mathrm{d}a}{\mathrm{d}u}$. (b) Modeling the dependence of the first-order correction $\Delta\left(\frac{\mathrm{d}a}{\mathrm{d}u}\right)$ by power law $\Delta\left(\frac{\mathrm{d}a}{\mathrm{d}u}\right) = Aa^n$ for some constant A. (c) Modeling the first-order correction by the coefficient C in $\Delta\left(\frac{\mathrm{d}a}{\mathrm{d}u}\right) = \frac{(1-C)\sigma}{a^2}$.

An exception would be the stationary solution which is studied in [1]. In this case, the inner layers are also very close to their Schwarzschild radii and the evaporation proceeds simultaneously. On the other hand, even in this case, although the inner layers completely evaporate first, the process is extremely slow because of the very large redshift factor, and the Hawking radiation mostly comes from the outer layers.

The inner layers stay frozen until the outer layers are evaporated. For an outer layer as close to the Schwarzschild radius as $R_n - a_n \sim \mathcal{O}(\sigma/a_n)$, the redshift factor for the layer at a separation ΔR under the outer surface is of order $\mathrm{e}^{-R_0\Delta R/2\sigma}$. Therefore, roughly speaking, it is natural to think of a layer of matter to have the thickness of a Planck length, and the layer is evaporated before the next layer starts to evaporate.

We also check the issue of stability for the large-slope configurations as we did for the small-slope configurations above. The transition process towards the asymptotic states is shown via the time-dependence of the masses of different shells. See figures 13 and 14. For both $\frac{\mathrm{d}a}{\mathrm{d}r} = \infty$ and $\frac{\mathrm{d}a}{\mathrm{d}r} = 10$, the first-order correction to the 0th-order Hawking radiation is also very small (see figures 15 and 16), as the case of small slopes.

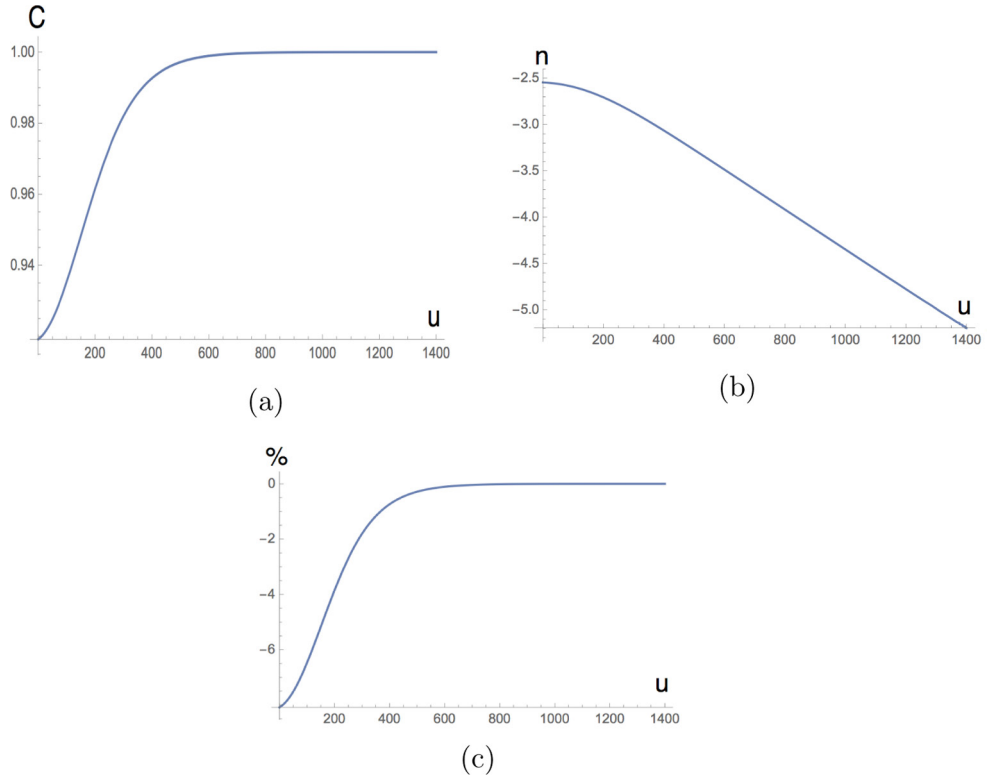

Figure 16. 1st-order correction in Hawking radiation for $\frac{da}{dr} = 10$. (a) The first-order correction $\Delta\left(\frac{da}{du}\right)$ as percentage of the 0th-order expression of $\frac{da}{du}$. (b) Modeling the dependence of the first-order correction $\Delta\left(\frac{da}{du}\right)$ by power law $\Delta\left(\frac{da}{du}\right) = Aa^n$ for some constant A. (c) Modeling the first-order correction by the coefficient C in $\Delta\left(\frac{da}{du}\right) = \frac{(1-C)\sigma}{a^2}$.

7. Discussion and conclusion

In this paper, we studied the dynamical process of collapsing spheres in the KMY model, in which the Schwarzschild radii are time-dependent due to the back-reaction of Hawking radiation.

First, we note that, while an ideal thin shell does not completely evaporate in the KMY model, a pseudo thin shell does. The origin of this over-sensitivity on short-distance features is the higher derivatives needed to determine Hawking radiation. By properly treating the higher-derivative terms (in a way analogous to how the Abraham–Lorentz formula is applied to point charges), the discrepancy between the ideal thin shell and pseudo thin shell disappears. All smooth configurations evaporate completely within finite time.

Secondly, we showed that there are two classes of asymptotic states in the KMY model. Their initial states are separated by a critical energy density ρ_c (50). When the initial energy density is much higher than the critical energy density, the collapsing shell approaches a thin shell state. If the initial energy density is much lower than ρ_c, the collapsing shell approaches a slope-1 configuration.

To approach the slope-1 configuration, the initial density of the matter has to be smaller than Hawking radiation, which is, for a large range of black-hole masses, much smaller than that of the current CMB. Therefore, the outer layers of black holes at present are expected to resemble a (pseudo) thin shell configuration.

Despite the apparent difference between the profiles of the slope-1 states and the thin shell states, both configurations appear to be very similar from the viewpoint of a distant observer. The reason is that the matter at a Planck length under the surface of the shell is essentially frozen [7]. It will be interesting to investigate how these asymptotic states can be distinguished by certain high-precision observations.

Similarly, the difference between either of the two asymptotic states and the conventional model of a black hole with a horizon is very small to a distant observer due to the huge redshift factor. How to distinguish the KMY model and the conventional model of black holes is a very interesting and important question. The most salient feature of the KMY model is the Planckian scale pressure under the surface of the collapsing matter, which is at a Planck-scale distance above the incipient horizon (hence the horizon will not appear). In contrast, the near-horizon region of a black hole in the conventional model is usually assumed to be empty. This difference is expected to be reflected in the gravitational wave signal for black-hole mergers. The gravitational wave signal of black-hole mergers has not yet confirmed the existence of the horizon [41, 42], while future gravitational wave observations with greater precision may be able to distinguish the KMY model and the conventional model [43, 44].

It should be noted that we have assumed that the gravitational force dominates over other forces in the gravitational collapse and that the collapsing matter is close to the speed of light, while the pressure of the matter is negligible (except for that from the quantum effect). For example, neutron stars have strong Fermi degeneracy pressure to resist the gravitational force. Thus the black hole formed by the gravitational collapse of a star has a minimal mass around a few solar masses. In this paper, we have assumed that the collapsing matter does not have such a large pressure which can stop the collapse.

Acknowledgment

The author would like to thank Heng-Yu Chen, Yi-Chun Chin, Chong-Sun Chu, Yu-tin Huang, Hsien-chung Kao, Hikaru Kawai, Ioannis Papadimitriou, Piljin Yi and Yuki Yokokura, for discussions. The work is supported in part by the Ministry of Science and Technology, R.O.C. and by National Taiwan University. The work of YM is also supported in part by JSPS KAKENHI Grants No. JP17H06462.

Appendix. Derivative expansion of collapsing shells

Here we verify that, under certain assumptions about the asymptotic limit, the slope-1 shells of an arbitrary thickness (including the pseudo thin shell) are the only lowest-order solutions in the derivative expansion of the formulas of Hawking radiation. The equations of Hawking radiation in the KMY model are equations (6), (9), (13) and (18). The lowest-order approximation of equation (9) is[8]

$$\{u, U\} \simeq \frac{1}{3}\dot{\psi}_0^2. \tag{A.1}$$

[8] There is, in fact, an ambiguity in the derivative expansion depending on which variable (ψ_0 versus $\mathrm{d}U/\mathrm{d}u$) is used.

First of all, it should be clear that the Hawking radiation is dominated by the contributions of those layers in the collapsing shell which are very close to their Schwarzschild radii. It is also obvious that, in terms of the coordinate u suitable for a distant observer, these layers spend a very long time approaching their Schwarzschild radii. The assumption we make is that the distribution of these layers eventually approach a certain universal asymptotic profile

$$R(a) - a \simeq f(a) \tag{A.2}$$

for a certain given function $f(a)$ that depends only on a and other physical constants. As the only relevant constant parameter in this model is σ (or $\kappa\mathcal{N}$), $f(a)$ can always be rewritten as $ag(\sigma/a^2)$ for a certain function g. Since σ/a^2 is an extremely tiny number, it is dominated by the leading-order term in its power expansion in σ/a^2. Therefore, we assume that

$$R(a) - a \simeq \frac{C}{a^n} \tag{A.3}$$

at the leading-order in the (σ/a^2)-expansion for a constant C and a number n. (This assumption excludes ideal thin shells.) A generic consequence of this is that

$$\dot{R}(a) - \dot{a} \simeq 0 \tag{A.4}$$

at the leading order. Taking u-derivatives on this equation and using equation (13), we find

$$\dot{a}_0 \simeq \dot{R}_0 \simeq -\frac{R_0 - a_0}{2R_0} \simeq -\frac{C}{2a_0^{n+1}}. \tag{A.5}$$

According to equation (6),

$$\psi_0 \simeq -\frac{a_0^{n+1}}{(n+1)C}. \tag{A.6}$$

Then equations (18) and (A.1) imply

$$\dot{a}_0 \simeq -\frac{\kappa\mathcal{N}}{12\pi}\dot{\psi}_0^2 \simeq -\frac{\kappa\mathcal{N}}{12\pi}\frac{a_0^{2n}}{C^2}\dot{a}_0^2, \tag{A.7}$$

from which we find

$$\dot{a}_0 \simeq -\frac{12\pi}{\kappa\mathcal{N}}\frac{C^2}{a_0^{2n}}. \tag{A.8}$$

The agreement between equations (A.5) and (A.8) demands that

$$n = 1, \tag{A.9}$$

$$C = \frac{\kappa\mathcal{N}}{24\pi}. \tag{A.10}$$

Therefore the asymptotic profile (A.3) is precisely the slope-1 configuration (without restriction on its thickness so pseudo thin shells are included). For the self-consistency of this result, one can check that the higher-order terms ignored in equation (A.1) are indeed much smaller than the lower-order terms.

ORCID iDs

Pei-Ming Ho https://orcid.org/0000-0002-0466-0351
Yoshinori Matsuo https://orcid.org/0000-0002-1742-6353

References

[1] Kawai H, Matsuo Y and Yokokura Y 2013 A self-consistent model of the black hole evaporation *Int. J. Mod. Phys.* A **28** 1350050
[2] Kawai H and Yokokura Y 2015 Phenomenological description of the interior of the Schwarzschild black hole *Int. J. Mod. Phys.* A **30** 1550091
[3] Ho P M 2015 Comment on self-consistent model of black hole formation and evaporation *J. High Energy Phys.* JHEP1508(2015) 096
[4] Kawai H and Yokokura Y 2016 Interior of black holes and information recovery *Phys. Rev.* D **93** 044011
[5] Ho P M 2016 The absence of horizon in black-hole formation *Nucl. Phys.* B **909** 394–417
[6] Baccetti V, Mann R B and Terno D R 2019 Trapped surfaces, energy conditions, and horizon avoidance in spherically-symmetric collapse *15th Marcel Grossmann Meeting on Recent Developments in Theoretical and Experimental General Relativity, Astrophysics, and Relativistic Field Theories (MG15)*
[7] Ho P M 2017 Asymptotic black holes *Class. Quantum Grav.* **34** 085006
[8] Kawai H and Yokokura Y 2017 A Model of black hole evaporation and 4D Weyl anomaly *Universe* **3** 51
[9] Russo J G, Susskind L and Thorlacius L 1992 The endpoint of Hawking radiation *Phys. Rev.* D **46** 3444
[10] Hajicek P 1987 On the origin of Hawking radiation *Phys. Rev.* D **36** 1065
[11] Parentani R and Piran T 1994 The internal geometry of an evaporating black hole *Phys. Rev. Lett.* **73** 2805
[12] Banerjee A, Chatterjee S and Dadhich N 2002 Spherical collapse with heat flow and without horizon *Mod. Phys. Lett.* A **17** 2335
[13] Vachaspati T, Stojkovic D and Krauss L M 2007 Observation of incipient black holes and the information loss problem *Phys. Rev.* D **76** 024005
[14] Paranjape A and Padmanabhan T 2009 Radiation from collapsing shells, semiclassical backreaction and black hole formation *Phys. Rev.* D **80** 044011
[15] Mersini-Houghton L 2014 Backreaction of Hawking radiation on a gravitationally collapsing star I: black holes? *Phys. Lett.* B **738** 61
[16] Mersini-Houghton L and Pfeiffer H P 2014 Back-reaction of the Hawking radiation flux on a gravitationally collapsing star II (arXiv:1409.1837 [hep-th])
[17] Baccetti V, Mann R B and Terno D R 2018 Role of evaporation in gravitational collapse *Class. Quantum Grav.* **35** 185005
[18] Ho P M and Matsuo Y 2018 On the near-horizon geometry of an evaporating black hole *J. High Energy Phys.* JHEP07(2018)047
[19] Ho P M, Matsuo Y and Yang S J 2019 Vacuum energy at apparent horizon in conventional model of black holes (arXiv:1904.01322 [hep-th])
[20] Bardeen J M 2014 Black hole evaporation without an event horizon (arXiv:1406.4098 [gr-qc])
[21] Ho P M and Matsuo Y 2019 Trapping horizon and negative energy *J. High Energy Phys.* JHEP06(2019)057
[22] Mathur S D 2009 The Information paradox: a pedagogical introduction *Class. Quantum Grav.* **26** 224001
[23] Almheiri A, Marolf D, Polchinski J and Sully J 2013 Black holes: complementarity or firewalls? *J. High Energy Phys.* JHEP02(2013)062
Braunstein S L 2009 Black hole entropy as entropy of entanglement, or it's curtains for the equivalence principle (arXiv:0907.1190v1 [quant-ph])
Braunstein S L, Pirandola S and Życzkowski K 2013 Better late than never: information retrieval from black holes *Phys. Rev. Lett.* **110** 101301 (published as Braunstein *et al*, for a similar prediction from different assumptions)

[24] Davies P C W, Fulling S A and Unruh W G 1976 Energy momentum tensor near an evaporating black hole *Phys. Rev.* D **13** 2720
[25] Arderucio-Costa B and Unruh W 2018 *Phys. Rev.* D **97** 024005
[26] Mann R B, Nagle I and Terno D R 2018 Transition to light-like trajectories in thin shell dynamics *Nucl. Phys.* B **936** 19
[27] Gerlach U H 1976 The mechanism of black body radiation from an incipient black hole *Phys. Rev.* D **14** 1479
[28] Stephens C R, 't Hooft G and Whiting B F 1994 Black hole evaporation without information loss *Class. Quantum Grav.* **11** 621
[29] 't Hooft G 1996 The scattering matrix approach for the quantum black hole: an overview *Int. J. Mod. Phys.* A **11** 4623
[30] Lunin O and Mathur S D 2002 AdS/CFT duality and the black hole information paradox *Nucl. Phys.* B **623** 342
Lunin O and Mathur S D 2002 Statistical interpretation of Bekenstein entropy for systems with a stretched horizon *Phys. Rev. Lett.* **88** 211303
[31] Barcelo C, Liberati S, Sonego S and Visser M 2008 Fate of gravitational collapse in semiclassical gravity *Phys. Rev.* D **77** 044032
[32] Kruger T, Neubert M and Wetterich C 2008 Cosmon lumps and horizonless black holes *Phys. Lett.* B **663** 21
[33] Yi S 2011 Black hole: never forms, or never evaporates *J. Cosmol. Astropart. Phys.* JCAP01(2011)031
[34] Fayos F and Torres R 2011 A quantum improvement to the gravitational collapse of radiating stars *Class. Quantum Grav.* **28** 105004
[35] Saini A and Stojkovic D 2015 Radiation from a collapsing object is manifestly unitary *Phys. Rev. Lett.* **114** 111301
[36] Baccetti V, Mann R B and Terno D R 2017 Do event horizons exist? *Int. J. Mod. Phys.* D **26** 1743008
[37] Davies P C W and Fulling S A 1976 Radiation from a moving mirror in two-dimensional space-time conformal anomaly *Proc. R. Soc.* A **348** 393
[38] Griffiths D J 1981 *Introduction to Electrodynamics* (Cambridge: Cambridge University Press)
[39] Yang C N and Feldman D 1950 The S matrix in the Heisenberg representation *Phys. Rev.* **79** 972
[40] Cheng T C, Ho P M and Yeh M C 2002 Perturbative approach to higher derivative and nonlocal theories *Nucl. Phys.* B **625** 151
Cheng T C, Ho P M and Yeh M C 2002 Perturbative approach to higher derivative theories with fermions *Phys. Rev.* D **66** 085015
[41] Abramowicz M A, Kluzniak W and Lasota J P 2002 No observational proof of the black hole event-horizon *Astron. Astrophys.* **396** L31
[42] Cardoso V, Franzin E and Pani P 2016 Is the gravitational-wave ringdown a probe of the event horizon? *Phys. Rev. Lett.* **116** 171101
Cardoso V, Franzin E and Pani P 2016 *Phys. Rev. Lett.* **117** 089902 (erratum)
[43] Cardoso V, Hopper S, Macedo C F B, Palenzuela C and Pani P 2016 Gravitational-wave signatures of exotic compact objects and of quantum corrections at the horizon scale *Phys. Rev.* D **94** 084031
[44] Abedi J, Dykaar H and Afshordi N 2017 Echoes from the Abyss: tentative evidence for Planck-scale structure at black hole horizons *Phys. Rev.* D **96** 082004